arXiv:2504.08930v2 [cs.LG] 25 Aug 2025

VectorLiteRAG: Latency-Aware and Fine-Grained Resource Partitioning for Efficient RAG

Junkyum Kim and Divya Mahajan

Georgia Institute of Technology

***Abstract*—Retrieval-Augmented Generation (RAG) systems combine vector similarity search with large language models (LLMs) to deliver accurate, context-aware responses. However, co-locating the vector retriever and the LLM on shared GPU infrastructure introduces significant challenges: vector search is memory- and I/O-intensive, while LLM inference demands high throughput and low latency. Naive resource sharing often leads to severe performance degradation, particularly under high request load or large index sizes.**

We present VECTORLITERAG, a deployment-friendly RAG system that achieves latency-compliant inference without requiring additional hardware resources. VECTORLITERAG introduces a fine-grained GPU resource allocation mechanism based on detailed performance modeling and access pattern analysis. By estimating search latency and query hit rate distributions, it identifies an optimal index partitioning point across CPU and GPU tiers to minimize contention and maximize throughput.

Our evaluations show that VECTORLITERAG consistently expands the SLO-compliant request rate range across all tested configurations, including both small and large LLMs, and small and large vector databases compared to naive baselines and state-of-the-art alternatives. In the best case, VECTORLITERAGimproves the attainable SLO throughput by up to 1.5× without compromising generation quality or requiring additional compute resources.

I. INTRODUCTION

Retrieval-Augmented Generation has emerged as a powerful system in natural language processing, particularly for domain-specific question answering and information retrieval tasks [9], [21], [31]. Its key strength lies in combining parametric memory, encoded in the weights of a large language model, with non-parametric memory retrieved from an external knowledge corpus. Although parametric memory provides strong generalization, it is expensive to train and difficult to update. To mitigate this, RAG pipelines first perform similarity search using approximate nearest neighbor search (ANNS) algorithms to retrieve relevant documents from a large database. The retrieved documents are then fed into the LLM's context to generate up-to-date and reliable responses.

RAG frameworks [19], [23], [36] typically adopt heterogeneous hardware configurations, where vector retrieval is executed on CPUs and LLM generation is served by GPUs. This division is driven by workload characteristics: LLM inference requires massive matrix multiplications and benefits significantly from GPU acceleration, while retrieval has traditionally been seen as a lighter task suited for CPUs. Offloading retrieval to CPUs allows GPUs to be dedicated to the more compute-intensive generation phase. CPU-based vector search may be sufficient for small vector databases. However, as the dimensionality of the embeddings and the size of the dataset grow, retrieval becomes increasingly compute- and memory-bound. CPUs, with limited parallelism, narrower vector units, and lower memory bandwidth, struggle to handle high-throughput similarity search at scale.

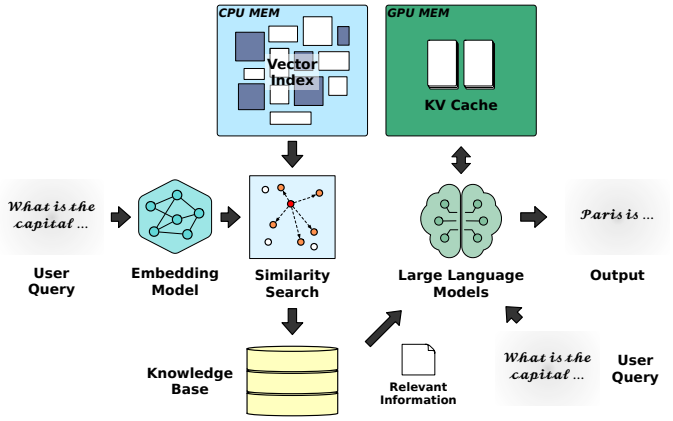

Fig. 1. End-to-end pipeline of a RAG system, where the input query is indexed into the vector database stored in memory, while the knowledge corpus resides in storage. The LLM prefill and decode execute on the GPU.

This latency imbalance creates a bottlenecked pipeline where the relatively slow CPU-based retrieval delays the GPU-accelerated generation phase, reducing the benefits of fast LLM inference and degrading overall system responsiveness. In our observations, CPU-based retrieval can take up to twice as long as the LLM prefill phase, increasing the total Time-to-First-Token (TTFT) from 197ms to 606ms when using a large database with 128M vectors, compared to a language model (Llama3-8B) operating without retrieval.

Although the retrieval operation is computationally lighter than the generation phase, it can still benefit significantly from GPU acceleration for two reasons: (1) GPUs feature wide and powerful vector units that enable highly parallelized distance computations, offering superior performance for similarity calculations on long embedding vectors. (2) The retrieval process involves scanning intermediate distance tensors to identify the closest data points in the vector space. These operations are typically implemented as memory lookups a task where GPUs outperform CPUs due to their vectorized memory access and higher I/O throughput.

In addition to compute and bandwidth demands, vector

retrieval introduces significant memory pressure. To reduce memory footprint and speed up the search process, vector databases are commonly compressed into vector indexes using quantization techniques such as product quantization (PQ) [12]. Nevertheless, even after compression, vector indexes still occupy significant memory space, often exceeding the memory capacity of a GPU. Furthermore, intermediate data structures such as distances between cluster centroids and queries consume additional memory.

These compute and memory pressures create a resource tension between the retrieval and generation stages, especially as the vector database grows and CPU-based search fails to meet strict latency requirements. GPU memory is already constrained, with most of it reserved for model weights and KV cache for the LLM. Naively sharding the vector index across all GPUs can lead to memory contention and reduced overall throughput. Alternatively, assigning a disaggregated GPU for retrieval can prevent direct interference between stages, but may degrade overall system throughput by reducing the number of available LLM instances, in particular when models require multiple GPUs, enforcing rigid allocation schemes. Motivated by these challenges, this work explores a holistic approach to optimizing distributed RAG pipelines through joint resource allocation between vector search and LLM generation. We present VECTORLITERAG, a system that partitions the vector index between GPU and CPU based on query access patterns and LLM deployment configurations, aiming to maximize throughput while meeting latency targets by exploiting the compute power of GPUs across both stages of the RAG pipeline. By analytically modeling similarity search latency, we determine the smallest index portion that needs to be placed on the GPU to satisfy the latency requirement under a given system configuration. Accordingly, VECTORLITERAG offers a latency-aware, throughput-optimized solution that requires no additional hardware resources. This approach is grounded in two key insights:

Access-Skew-Aware Data Layout. VECTORLITERAG leverages a key characteristic of IVF-based retrieval systems, that query accesses exhibit skew across clusters. To take advantage of this, VECTORLITERAG introduces an analytical model that determines the optimal partitioning point and corresponding layout for a multi-GPU system. While the coarse quantizer and cold clusters remain on the CPU, a small subset of hot clusters are cached and distributed across GPUs. The system allocates just enough hot clusters to the GPUs, avoiding both oversubscription of GPU resources during retrieval.

Inter/Intra-Query Variance-Aware Routing. Hit rates vary across queries and, within a single query, across devices. Static retrieval configurations, such as fixed search budgets per device, fail to capture this variance and often result in unnecessary allocation of GPU thread resources. VECTORLITERAG addresses this by incorporating query and device-level awareness into its task routing and resource allocation. After identifying the most relevant clusters, retrieval tasks are dispatched to GPUs or CPUs based on their expected contribution to overall search task. Moreover, by monitoring query progress during retrieval, VECTORLITERAG opportunistically forwards early-completing queries to the LLM stage, reducing synchronization delays caused by straggler queries and improving latency under batching.

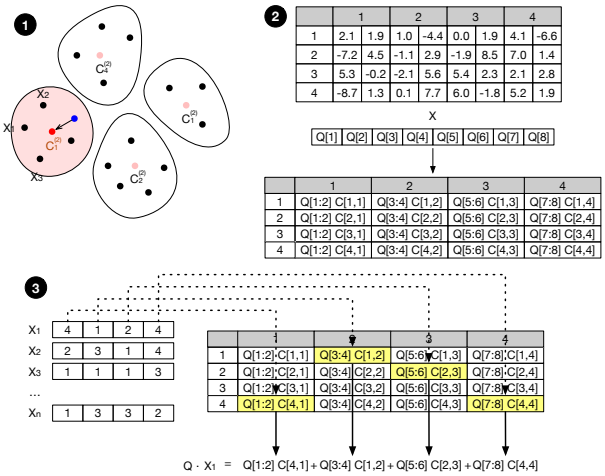

Fig. 2. Three stages of vector search in IVF–based index: (1) coarse quantization to identify clusters most semantically similar to the query, (2) construction of a LUT containing partial distances between the query and codewords, and (3) scanning the LUT and re-ranking candidates from the selected clusters based on aggregated distances.

Our contributions are summarized as follows:

- Identifies and models access skew in IVF-based retrieval systems and proposes a hit rate estimation method based on observed cluster access patterns.
- Develops an analytical latency model that predicts retrieval time while accounting for inter-query hit rate variance. Using this model, VECTORLITERAGdetermines an optimal index partitioning point that satisfies latency targets.
- Designs a distributed retrieval pipeline that adaptively allocates search tasks across CPUs and GPUs by exploiting inter-device hit rate variance, thereby improving efficiency and avoiding unnecessary GPU resource usage.

II. RETRIEVAL AUGMENTED GENERATION

The Retrieval-Augmented Generation pipeline combines information retrieval with LLM inference to enable efficient, context-sensitive response generation [7], [8], [21]. User queries are first transformed into vector embeddings using embedding models [28], [32], [34], [39]. These embeddings capture the semantics of the input and enable similarity search by comparing query vectors to a vector database constructed from the knowledge corpus.

Since exhaustive pairwise search is computationally infeasible at scale, large-scale vector retrieval relies on approximate nearest neighbor search to efficiently identify relevant documents. The retrieved vectors are mapped back to their corresponding documents, which are provided as additional context to the LLM alongside the original query.

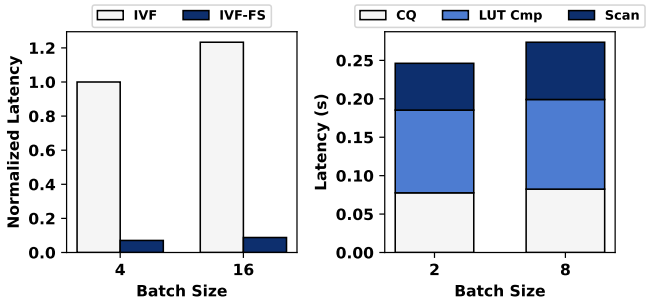

Fig. 3. **Left**: Search latency comparison between standard IVF and IVF with fast scan (IVF-FS). Except for the fast scan optimization, both indexes share identical configurations. IVF-FS achieves significantly faster search speed. **Right**: Latency breakdown of IVF-FS on a 128M vector index. Lookup table operations dominate the overall search time.

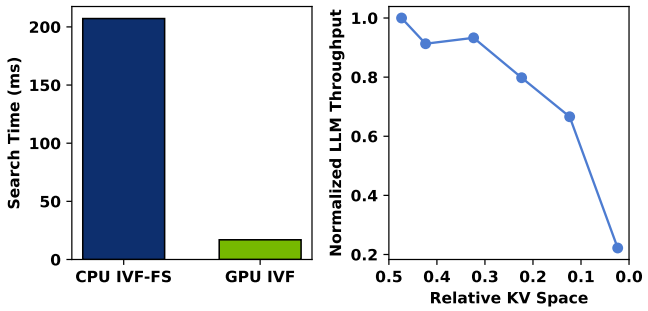

Fig. 4. **Left**: While fast scanning accelerates IVF-based vector search on CPU(64 core Xeon 8462Y+), GPU(H100)-based IVF search offers superior performance. **Right**: Relationship between KV cache size and LLM throughput for the Qwen3-30B model on two H100 GPUs. Reducing KV cache space leads to a significant drop in throughput.

A. Inverted List Index IVF

There are several approaches for structuring a vector database into a searchable index. Among them, HNSW and IVF are the most widely used.

HNSW [25] (Hierarchical Navigable Small World) is a graph-based structure where each vector forms a node connected to its nearest neighbors. It enables rapid search via hierarchical traversal and offers fast index construction. However, the additional edge information significantly increases memory usage as the dataset grows.

The Inverted File (IVF) index [43], by contrast, organizes the index as a hierarchical clustering structure. A subset of vectors is first clustered via k-means to obtain centroids. Then, each database vector is assigned to the closest centroid, forming an inverted list. This structure narrows the search space using only centroid metadata, resulting in low memory overhead and high scalability. As such, IVF is widely adopted and studied in retrieval systems for large knowledge corpora [5], [10], [13], [20], [33], [40].

To further reduce memory usage, quantization techniques are applied on top of IVF. Scalar quantization (SQ) reduces each vector element to a smaller numerical type (e.g., `float32` to `int8`), offering simplicity but limited compression. For higher compression ratios, product quantization (PQ) [12] is commonly used.

B. Search Operation in IVF Index

Figure 2 illustrates the search process in an IVF-PQ index, where an inverted list structure is combined with product quantization. When a query is received, the retriever first identifies the closest clusters, narrowing the search space. The number of clusters searched is controlled by the parameter `nprobe`, which trades off speed and accuracy.

Next, a distance lookup table is constructed. Since each vector is quantized into discrete sub-vector codes, each code maps to a representative value, trained and stored in the codebook. By pre-computing distances between the query vector and these representative values, the system avoids computing full distances to every vector. During the scan stage, these LUTs are used to accumulate approximate distances and retrieve the top-k nearest vectors.

A deeper analysis of IVF search, shown in Figure 3, reveals that the large portion of the search time is spent on constructing and scanning the distance lookup table. This highlights the LUT stage as a key bottleneck in retrieval latency. To mitigate this overhead, fast scanning techniques [3] have been proposed and implemented in libraries such as Faiss [5] and ScaNN [40]. These methods leverage SIMD instructions and CPU vector registers to accelerate distance lookup operations. By carefully organizing lookup tables and quantization codes into memory-aligned layouts, they significantly outperform conventional IVF scan routines, particularly in CPU-based environments.

Motivated by their superior latency-performance trade-off, we adopt fast scanning in our system to enable efficient and low-latency vector retrieval. However, despite the SIMD capabilities of modern CPUs, CPU-based search can still become a bottleneck, ultimately degrading the responsiveness of the RAG system.

III. Challenges and Opportunities in RAG Serving

A. GPU search vs. CPU search

While fast scan indexes significantly improve the latency of vector similarity search on CPUs, GPU-based retrieval can offer even greater speedups, thanks to their wider vector processing units and higher memory bandwidth. As shown in Figure 4 (left), GPU-accelerated IVF search can outperform fast scan methods by nearly an order of magnitude.

Thus, offloading retrieval to the GPU becomes appealing for large-scale vector databases where CPU-based search remains a bottleneck. However, this comes with a fundamental trade-off: GPU memory is already heavily utilized by LLMs, particularly for storing KV cache and model weights. Allocating additional memory for the vector index can reduce available cache space, ultimately degrading LLM throughput, as illustrated in Figure 4 (right).

Beyond memory capacity, GPU retrieval also incurs overheads in compute resource scheduling. Shared memory is used to stage partial distance lookup tables, and each query–cluster

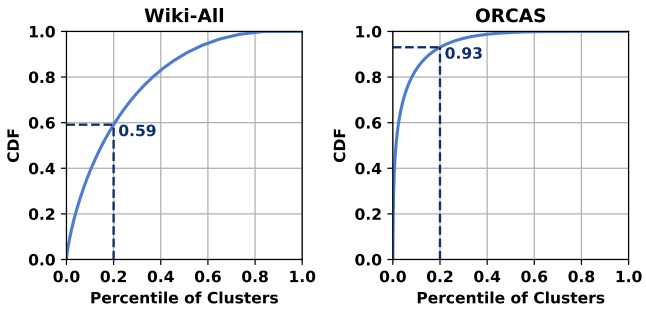

Fig. 5. CDF of cluster access frequency for queries from the Wiki-All [35] and ORCAS [4] datasets. While the two distributions exhibit different levels of skewness, in both cases, the top 20% of clusters account for over 50% of the total distance computations.

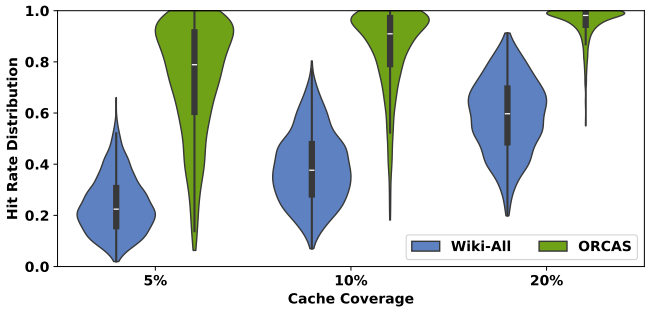

Fig. 6. Hit rates vary significantly across queries, and even when the average hit rate is high, long-tail queries with low hit rates persist. This is particularly evident in the ORCAS dataset.

pair typically maps to a thread block. As the number of probed clusters increases, so does the occupancy and scheduling pressure on the GPU, further impacting performance.

Takeaway 1. ***GPU-based retrieval can substantially outperform even the fastest CPU-based methods, but due to contention with LLM inference workloads, careful memory and compute allocation is essential.***

B. Opportunity of Tiered Search Structure

The distribution of query access patterns in IVF indexes reveals the presence of hot clusters, a small subset that dominates retrieval traffic.

As shown on the left of Figure 5, the cumulative distribution of coarse quantization results exhibits a strong skew: the top 20% of clusters account for nearly 60% of accesses in Wiki-All [35] and over 93% in ORCAS [4]. This skew is especially pronounced in ORCAS, which reflects real-world query behavior through unfiltered click-through logs, capturing both popularity bias and the imbalance introduced by k-means quantization.

This imbalance results in inefficient memory usage, as significant resources are allocated to rarely accessed clusters with limited contribution to retrieval quality.

Takeaway 2. ***IVF index access patterns are highly skewed: a small number of clusters account for the vast majority of retrievals. This motivates a tiered index design, where frequently accessed clusters are prioritized for acceleration (e.g., GPU caching), and cold clusters are offloaded to lower-tier compute and storage.***

Embedding access patterns in recommendation systems are also known to exhibit significant skew, where a small subset of items or users dominates embedding lookup frequency. This observation has motivated several tiered architecture designs that prioritize popular embeddings for faster access [1], [2], [18], [27].

Inspired by this insight, our work applies a similar idea of tiered acceleration to vector similarity search. However, a key distinction lies in the granularity of retrieval: while recommendation systems typically involve individual embedding lookups, vector search systems such as those based on IVF retrieve and compare distances across hundreds to thousands of vectors per query. Thus, skew in our setting emerges more prominently at the *cluster* level rather than the vector level.

Consequently, although both domains benefit from tiered designs, the unit of optimization and the manifestation of skew differ substantially. Our approach focuses on cluster-level skew in large-scale retrieval workloads, complementing prior work in recommendation systems.

C. Variance of Hit Rate across Queries

While tiered resource allocation strategies can accelerate vector search by caching frequently accessed clusters, their effectiveness in deployment is often hindered by query-level variance in hit rates. In particular, long-tail queries with low cache coverage can significantly limit the overall performance gains.

Figure 6 presents a violin plot of hit rate distributions across queries, measured by counting the number of clusters (among the total `nprobe`) that fall within the cached hot cluster set. As cache coverage increases from 5% to 20% of total clusters, the average hit rate improves accordingly. However, the variance remains substantial, especially in highly skewed datasets such as ORCAS, where a long tail of queries exhibits minimal cache benefit.

This variance introduces a deployment challenge. Since vector search throughput scales with batch size, retrievers are typically deployed with batching enabled. However, in the presence of low-hit queries within a batch, the entire batch's processing time is effectively bounded by the slowest query. As a result, even if the average per-query latency is reduced by GPU acceleration, end-to-end latency improvements are constrained.

To fully realize the benefits of tiered or cached retrieval in real-world deployments, it is essential to account for such hit rate variance and long-tail behavior during system design.

Takeaway 3. ***Variance in hit rate across queries poses a challenge in latency-critical deployments, due to long-tail queries as batching amplifies the impact of long-tail queries, limiting the effectiveness of caching.***

In summary, while GPU-based retrieval can vastly outperform CPU methods, it introduces a resource contention prob-

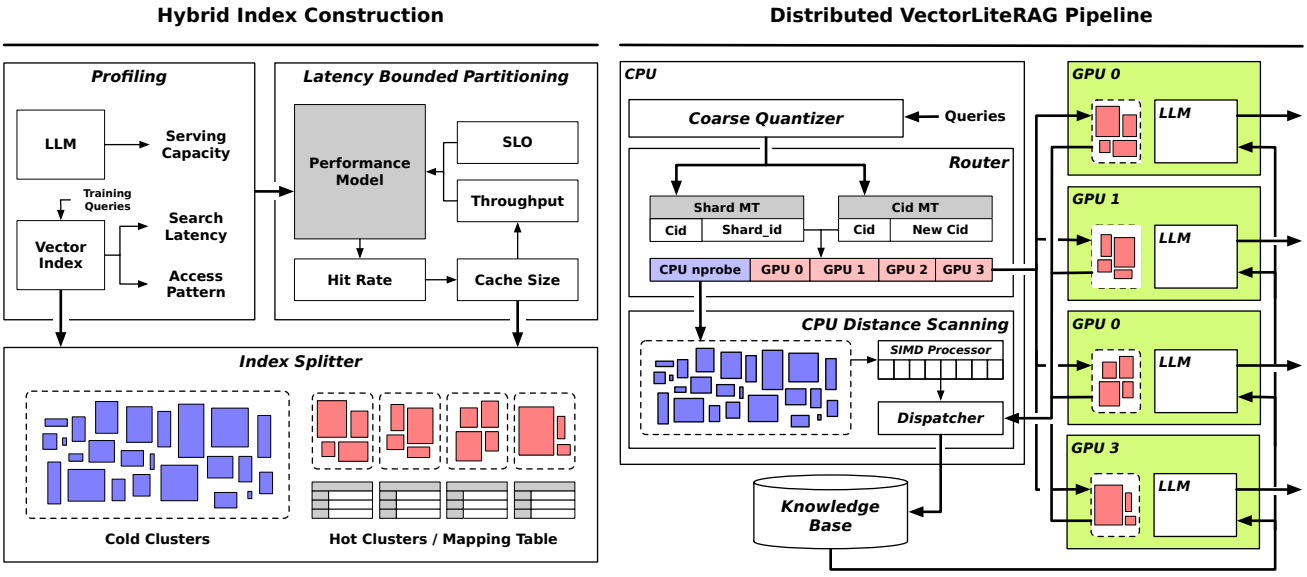

Fig. 7. System architecture of VECTORLITERAG. The system consists of two stages: offline Hybrid Index Construction (left) and runtime Distributed VECTORLITERAGPipeline (right). During index construction, profiling is conducted to model search latency, query access patterns, and LLM throughput. These are used in the latency-bounded partitioning module to determine the optimal cache size and index partitioning point. The index splitter then constructs sharded GPU/CPU indices and mapping tables. At runtime, queries are processed by a CPU-based coarse quantizer and routed to appropriate workers using mapping tables. Hot clusters are scanned on GPUs, while cold clusters are processed by CPU SIMD cores. A dynamic dispatcher collects early-finished queries and forwards them to LLM workers to reduce tail latency and improve batching efficiency.

lem when co-located with LLMs, due to limited GPU memory and compute capacity. Meanwhile, query access patterns exhibit strong skew: a small fraction of clusters account for the majority of retrieval traffic, making selective caching and tiered search strategies highly effective. However, significant variance in hit rates across queries especially the presence of long-tail queries, poses a major challenge in latency-sensitive deployments, as batching magnifies the performance bottleneck introduced by slow queries. These insights motivate VECTORLITERAG, a system that adaptively partitions the index across GPU and CPU tiers, accounting for workload skew, hit rate variance, and end-to-end latency constraints to optimize both throughput and responsiveness.

IV. VECTORLITERAG

VECTORLITERAG is an optimized RAG system that determines the optimal configuration for a CPU-GPU hybrid vector index. Given the latency constraint, LLM specification, vector index, and system configuration, it computes a partitioning point for tiered search, constructs the corresponding hybrid index, and serves inference requests on a tailored execution pipeline. Figure 7 illustrates the system architecture. VECTORLITERAG consists of two main stages: offline hybrid index construction and the runtime distributed pipeline.

Offline Hybrid Index Construction. This stage begins by profiling CPU-based vector search latency and the query-to-cluster access patterns. It also measures the standalone throughput capacity of the LLM to model contention dynamics. These profiles are used to build a performance model and a cache coverage estimator. Then, based on this model, a latency-bounded partitioning algorithm determines the optimal coverage of "hot" clusters to be placed on the GPU. The index is then partitioned accordingly, creating sharded sub-indexes for the CPU and GPU.

Distributed VECTORLITERAG Pipeline. At runtime, batched retrieval requests are routed to the appropriate CPU or GPU shards using mapping tables created during index splitting. This reduces the memory and compute pressure on each worker shard and mitigates resource contention with co-located LLM inference. To improve batching efficiency and reduce tail latency, we employ a dynamic dispatcher that proactively identifies early completed queries and forwards them to the next stage of the RAG pipeline.

V. HYBRID INDEX CONSTRUCTION

A. Profiling-based Performance Modeling

Since GPU resources are limited, accurately modeling system performance is critical for determining the optimal index partitioning point. To construct these models, VECTORLITERAG profiles latency and access statistics using calibration queries from a training set. Specifically, it collects: (1) latency breakdown of CPU-based vector search and (2) cluster access frequency distributions. Additionally, the standalone throughput of the LLM is measured to guide partitioning decisions under joint CPU-GPU execution.

As described in Section II-B, IVF index search latency is dominated by two components: coarse quantization (CQ) and LUT operations. We profile both stages across varying batch sizes and construct independent models for each. However, in our design, only the LUT stage is considered for GPU offloading, for two main reasons:

First, CQ is itself a similarity search over the quantizer (centroid) vectors, which is often implemented using memory-intensive graph-based structures such as HNSW. Offloading

CQ to GPU would require additional memory for the graph and complicate memory management. Second, if CQ were distributed across GPU shards, the resulting search path would involve repeated device transitions: CPU → GPU (quantization) → CPU (merge and routing) → GPU (search) → CPU (final merge). This induces costly inter-device communication and synchronization overheads. To avoid these complications, we retain CQ on the CPU and focus GPU optimization on LUT operations.

Empirically, as shown in Figure 8 (left), CPU search latency exhibits a piecewise linear relationship with batch size. Initial steps appear as the system transitions from single-threaded (single query) to multi-threaded execution (batched queries). Accordingly, we model $T_{\text{CQ}}^{\text{CPU}}$ and $T_{\text{LUT}}^{\text{CPU}}$ as piecewise linear functions of batch size.

When hot clusters are cached, overall search time reduces accordingly. In particular, since LUT operations offloaded to the GPU they are fully overlapped with the remaining CPU-side processing. As a result, we model the latency of the hybrid partitioned index as:

$$\tau_s(b) = T_{\text{CQ}}^{\text{CPU}}(b) + (1-\eta) \cdot T_{\text{LUT}}^{\text{CPU}}(b) \tag{1}$$

where η denotes the hit rate, more precisely the minimum hit rate among all queries in the batch.

B. Tail Query Hit Rate Estimation

As discussed in Section III-C, caching hot clusters leads to varying hit rates across queries. Since LUT workload is proportional to the number of clusters processed on the CPU $(1-\eta)$, this variance directly translates to latency differences.

To maximize throughput, vector search is typicall y executed in batches. However, batch-level search latency is dictated by the slowest, tail query. Therefore, modeling the minimum hit rate within a batch is critical for accurate performance estimation.

We model the distribution of per-query hit rates using a Beta distribution $f(x)$, which is widely used in Bayesian statistics to model random variables constrained between 0 and 1. Given a batch of size b, the expected minimum hit rate $\eta_{\min}$ (i.e., the first-order statistic) is computed as:

$$\eta_{\min}(B) = \int_0^1 B \cdot x \cdot f(x) \cdot (1 - F(x))^{B-1}\, dx \tag{2}$$

where $F(x)$ is the cumulative distribution function (CDF) of $f(x)$.

The mean hit rate $\bar{\eta}$ is easily derived from the query-cluster access frequency profile: the cumulative access percentage of cached clusters. Estimating the variance is more challenging, as it would require re-running queries through the quantizer and counting individual hits after masking hot clusters, a process that is both computationally expensive and incompatible with iterative partitioning algorithm.

Instead, we approximate the hit rate variance as a function of the mean. We observe that hit/miss heterogeneity is maximized when $\bar{\eta} = 0.5$, and becomes more uniform as $\bar{\eta} \to 0$ or $\bar{\eta} \to 1$.

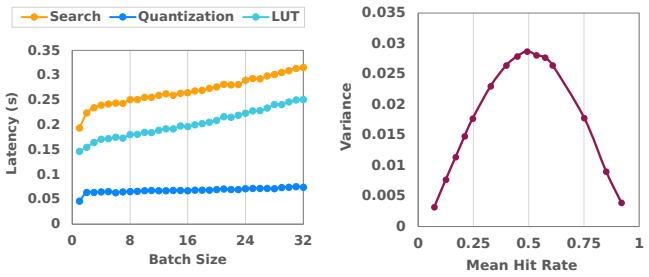

Fig. 8. **Left:** Search latency of ORCAS queries on a 64-core Intel Xeon 8426Y CPU. **Right:** Empirical variance of hit rates across queries in the Wiki-All dataset as a function of mean hit rate. The observed parabolic shape supports our variance approximation model.

This mirrors the variance behavior of the Beta distribution, where:

$$\text{Var}(X) \propto \bar{\eta}(1-\bar{\eta})$$

Thus, by empirically profiling the variance at $\bar{\eta} = 0.5$, denoted $\sigma^2_{\max}$, we can approximate the variance at arbitrary $\bar{\eta}$ as:

$$\sigma^2 \approx 4 \cdot \sigma^2_{\max} \cdot \bar{\eta}(1-\bar{\eta})$$

Figure 8 (right) validates the approximation. This allows instantiating a Beta distribution with inferred mean and variance for any cache coverage configuration.

Finally, using Eq. 2, we compute the minimum hit rate within a batch for a given cache coverage. Inverting this relation numerically yields the function:

$$\rho = \textsc{HitRate2Coverage}(B, \eta_{\min})$$

which is used in the main partitioning algorithm to identify the optimal cache coverage that satisfies latency constraints.

C. Latency-Bounded Partitioning Algorithm

In proposed hybrid CPU-GPU RAG pipeline, LLM throughput is inversely related to vector index cache coverage, due to GPU memory contention between KV cache and index storage. To find the optimal balance, we propose an iterative algorithm that searches for the optimal index partitioning point.

Algorithm 1 outlines the proposed latency-bounded partitioning algorithm. It takes the following inputs: the latency target, the baseline KV cache memory footprint when no vector index is loaded, and the peak standalone LLM throughput. The goal is to determine the largest feasible GPU index cache coverage (partitioning point ρ) that satisfies the latency constraint.

We begin by computing the latency bound for the hybrid vector search stage. To account for queuing delay, we conservatively consider the worst-case scenario: a request arriving just after the previous batch has started processing. Under steady-state load with uniformly arriving requests, this tail query experiences the full batch latency $W(b)$ as queuing

delay. Hence, to ensure total response time remains within the latency budget, we bound the hybrid search latency as:

$$\tau_s = \text{SLO}_{\text{search}} - W(b) \tag{3}$$

To simplify analysis and avoid circular dependency (since $W(b)$ depends on τ_s), we approximate this using a queuing factor ϵ, leading to:

$$\tau_s = \frac{\text{SLO}_{\text{search}}}{1+\epsilon} \tag{4}$$

In our setting, we conservatively set $\epsilon = 1$, corresponding to the worst-case queuing delay equal to one batch latency.

Next, we perform binary search over possible values of ρ using the modeled latency and hit rate behavior.

Search iteration. For each candidate ρ, we first estimate the reduced LLM throughput due to decreased KV cache space. While this interpolation is coarse, it gives a conservative lower bound because the throughput–cache curve is generally convex. We then invoke the INFERPARTITION function. It computes the expected batch size as $B = \mu \cdot \tau_s$, where μ is the current throughput bound. Since batch size B must be an integer, we consider two rounding strategies:

- **Rounding up.** This implies longer latency and thus requires more cache coverage to meet τ_s. From the hybrid latency model (Eq. 1), we solve for η_1 and convert it to coverage ρ_1 via the HITRATE2COVERAGE function.

- **Rounding down.** This yields a smaller batch size (shorter latency), but may not meet the required throughput. To ensure throughput μ is met, we solve for η_2 using the adjusted latency bound B/μ from the throughput constraint.

We then select the smaller of ρ_1 and ρ_2 to minimize GPU memory usage. This value is used to update the binary search interval.

Convergence. If the new partitioning point ρ increases, the resulting decrease in throughput leads to a smaller batch size in the next iteration, pulling ρ back down. Conversely, if ρ shrinks, the throughput bound increases, allowing for more cache coverage. This feedback loop ensures convergence of the binary search within a small number of iterations.

In practice, the algorithm converges in under one minute and provides an optimal GPU–CPU partitioning point ρ that satisfies the latency target while preserving maximum LLM throughput.

D. Index Splitter

Once the partitioning point ρ is determined, it is passed to the final stage of index construction: the index splitter. The splitter first identifies the hot clusters based on the access profile and the target cache coverage ρ. These hot clusters are then sorted by size and distributed to GPU shards in a round-robin fashion to balance memory usage across sub-indexes.

Alongside the construction of each sub-index, the splitter generates a set of mapping tables. These tables encode the correspondence between original cluster IDs and their assigned shard as well as the remapped local cluster IDs, enabling efficient routing during query execution.

Algorithm 1 Latency Bounded Partitioning

Input: $\text{SLO}_{\text{search}}$, $MEM_{KVcache}$, μ_{LLM0}
Output: ρ

$\tau_s \leftarrow \frac{\text{SLO}_{\text{search}}}{1+\varepsilon}$
$\rho_{\text{low}} \leftarrow 0$, $\rho_{\text{high}} \leftarrow 1$
while $\rho_{\text{high}} - \rho_{\text{low}} > \delta$ **do**
  $\rho_m \leftarrow \frac{\rho_{\text{low}} + \rho_{\text{high}}}{2}$
  $\mu_{\text{LLM}} \leftarrow \frac{MEM_{KVcache} - MEM_{Index}(\rho)}{MEM_{KVcache}} \mu_{LLM0}$
  $\rho \leftarrow \text{INFERPARTITION}(t_s, \mu_{\text{LLM}})$
  if $\rho > \rho_m$ **then**
    $\rho_{\text{low}} \leftarrow \rho$
  else
    $\rho_{\text{high}} \leftarrow \rho_m$
  end if
end while
return ρ

function INFERPARTITION(τ_s, μ)
  $B \leftarrow \lceil \tau_s \cdot \mu \rceil$
  $T^{\text{CPU}}_{\text{search}}(B), T^{\text{CPU}}_{\text{LUT}}(B) \leftarrow \text{PERFMODEL}(B)$
  $\eta_1 \leftarrow \frac{T^{\text{CPU}}_{\text{search}}(B) - \tau_s}{T^{\text{CPU}}_{\text{LUT}}(B)}$
  $\rho_1 \leftarrow \text{HITRATE2COVERAGE}(\eta_1, B)$
  $B \leftarrow \lfloor \tau_s \cdot \mu \rfloor$
  $T^{\text{CPU}}_{\text{search}}(B), T^{\text{CPU}}_{\text{LUT}}(B) \leftarrow \text{PERFMODEL}(B)$
  $\eta_2 \leftarrow \frac{T^{\text{CPU}}_{\text{search}}(B) - B/\mu}{T^{\text{CPU}}_{\text{LUT}}(B)}$
  $\rho_2 \leftarrow \text{HITRATE2COVERAGE}(\eta_2, B)$
  return $\min(\rho_1, \rho_2)$
end function

VI. DISTRIBUTED VECTORLITERAG PIPELINE

The right side of Figure 7 illustrates the runtime architecture of VECTORLITERAG. Similar to other IVF-based indexes, the pipeline begins with coarse quantization to identify candidate clusters. From this point, however, VECTORLITERAG introduces a customized retrieval pipeline tailored for hybrid CPU-GPU execution. We now describe each component in detail.

1) Router: To support efficient retrieval on a distributed multi-GPU system, VECTORLITERAG implements a custom router rather than relying on Faiss's built-in `IndexIVFShards`. The default implementation in Faiss is suboptimal in constrained environments for two main reasons:

(1) `IndexIVFShards` partitions the index uniformly by vector or cluster ID, ignoring access frequency. While, convenient for implementation, it retains centroid metadata even for clusters that are not locally resident, causing unnecessary memory overhead, especially problematic when the number of clusters is large.

(2) During search, each sub-index is instructed to probe the same number of clusters, even if many of them are not

resident on that shard. Although certain probes are ultimately skipped at runtime, the batched execution of cluster scanning kernels still launches GPU thread blocks for them. These launches consume scheduling bandwidth and shared memory resources, regardless of whether the actual computation is needed. Since shared memory usage increases with `nprobe`, this results in inefficient kernel launches and exacerbates resource contention, especially in large-scale vector databases.

To address these issues, VECTORLITERAG uses the mapping tables generated during index splitting to compactly route each query to the appropriate GPU shards and prune irrelevant probes. As a result, the effective `nprobe` per shard is significantly reduced, lowering both memory and kernel scheduling overhead. At runtime, only GPU workers holding relevant clusters receive and execute the search request, while the remaining portion of the search is handled by the CPU. This hybrid execution minimizes contention and ensures efficient utilization of GPU memory and compute.

2) Dynamic Dispatcher: Because hit rates vary across queries, the effective `nprobe` differs even within a batch. As batch size increases, the minimum hit rate tends to decrease, elongating the search latency for the entire batch. To mitigate this issue, VECTORLITERAG employs a dynamic dispatcher that accelerates early query completion.

When search is initiated, a separate dispatcher thread is launched. Each GPU worker sets a completion flag once its assigned clusters are scanned. After all GPU flags are set, the dispatcher begins polling for queries that have completed their full search.

To facilitate timely query promotion, a callback mechanism connects the CPU search loop and the dispatcher. The CPU processes clusters one-by-one, grouped by related queries. At the end of each iteration, the current scan count is compared with the expected `nprobe` for each query. When all assigned clusters for a query are scanned, the callback is invoked, and the query and its results are inserted into a thread-safe queue.

The dispatcher polls this queue at short intervals. Once a completed query is available, it merges the CPU and GPU results, re-ranks them to obtain the final top-k vectors, and forwards the result to the downstream document retriever. This proactive execution reduces head-of-line blocking within batches and improves end-to-end latency, particularly for high-hit-rate queries. It also enhances batching continuity by enabling smoother transitions between retrieval and generation stages, which already employs continous batching schemes.

VII. METHODOLOGY

A. Experiment Setup

To evaluate VECTORLITERAG, we conduct experiments across various datasets, models, and hardware configurations. This section describes the datasets, models, evaluation metrics, and system setup.

Datasets and Models. We use two datasets: Wiki-All and ORCAS. IVF index was built following the configuration guide presented in the Faiss library. Wiki-All [35] contains 88M 768-dimensional vectors derived from Wikitext (Kaggle) [26] and Cohere Wikipedia embeddings, with a compressed IVF index occupying 18GB.

Additionally, we construct two indexes from chunked Wikipedia documents using the Stella [39] embedding model of dimensions 1024 and 2048, with queries sampled from the Microsoft ORCAS dataset [4]. ORCAS consists of real Bing queries and retains duplicates to capture realistic query distributions. The ORCAS 1K and ORCAS 2K indexes require 40GB and 80GB of memory, respectively.

Our retrieval pipeline builds on Faiss v1.9.0 [5], [16], with internal extensions for flexible `nprobe` settings and dispatcher callbacks. The system, including the profiler and latency-aware scheduler, is implemented in Python.

For generation, we use Llama3-8B, Qwen3-32B, and Llama3-70B [6], [38], served via vLLM v0.9.1 [17]. The retriever and LLM servers run as separate subprocesses, while the main process manages request generation and document fetching, enabling seamless integration of the end-to-end RAG pipeline.

To evaluate system performance, we sample queries from a dedicated test set that is disjoint from the profiling set. The request arrival process follows a Poisson distribution, a commonly adopted modeling choice in prior work [17], [29], [42]. For each query, the top-25 documents are retrieved, and a 1024-token input is constructed and passed to the LLM, which then generates a 256-token output, following the setup in [33]. The initial `nprobe` is set to 2048, which is sufficient to achieve a retrieval quality of 0.91 Normalized Discounted Cumulative Gain (NDCG) [37] at 50.

SLO Settings. The SLOs for retrieval and generation stages were defined separately and then combined. For retrieval, since no standard criteria exist, we set the SLOs heuristically, relaxing them for larger databases (see Table I). For generation, the SLO was defined as the latency measured at the model's throughput limit. These capacity values were also used in building our performance model.

Vector Index	SLO_{search}	**LLM**	SLO_{LLM}
Wiki-All	150ms	Llama3-8B	217ms
ORCAS 1K	200ms	Qwen3-32B	191ms
ORCAS 2K	300ms	Llama3-70B	311ms

TABLE I
LATENCY REQUIREMENT OF EACH STAGE USED IN THE EVALUATION

System Configuration. Experiments were conducted on two types of nodes, each equipped with eight NVIDIA GPUs. The L40S node includes L40S GPUs with 48GB GDDR memory and dual Xeon 6426Y CPUs. The H100 node uses H100 GPUs with 80GB HBM and Xeon Platinum 8462Y CPUs. We used the L40S node for smaller models (Llama3-8B), while larger models requiring model parallelism (Qwen3-32B, Llama3-70B) were run on the H100 node for maximum throughput.

Baseline Configurations. We compare VECTORLITERAG against several key baselines. Since VECTORLITERAG builds on FAISS, we use vanilla FAISS-CPU IVF FastScan (CPU-Only), FAISS-GPU IVF on a dedicated GPU (DED-GPU), and a sharded FAISS-GPU IVF index distributed across all GPUs (ALL-GPU). To further demonstrate the strength of our

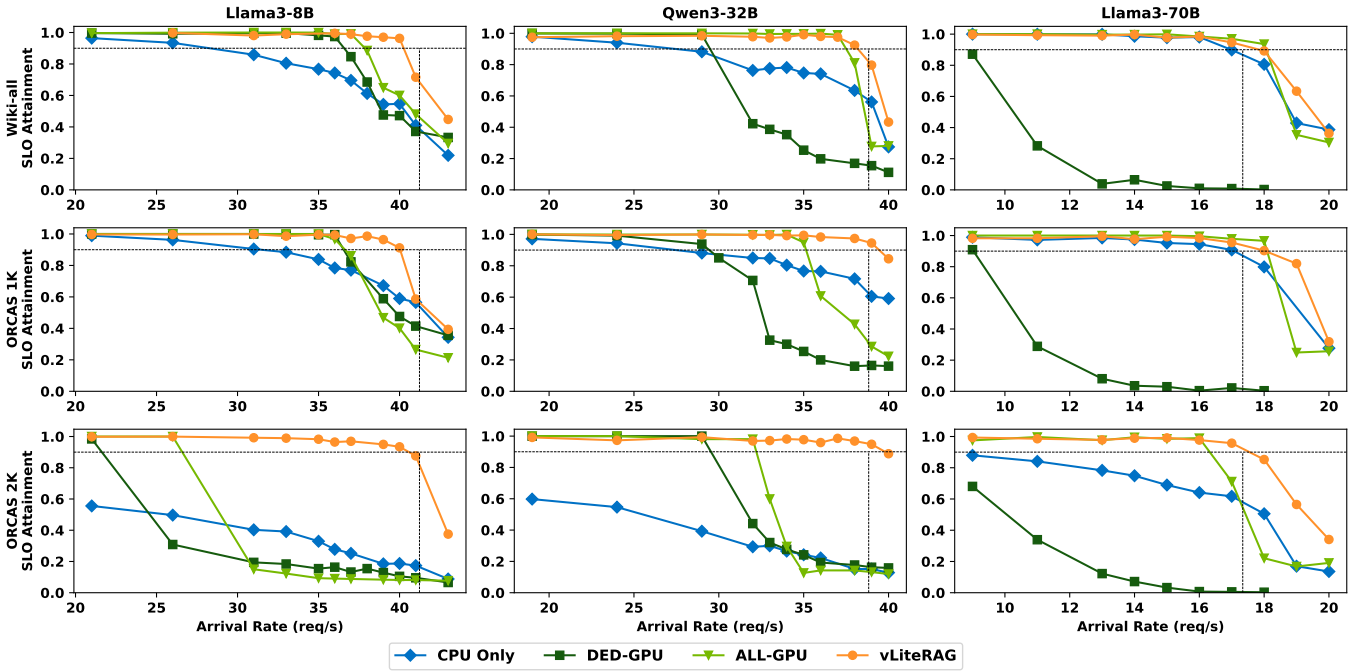

Fig. 9. TTFT SLO attainment of RAG pipeline under increasing arrival rates across different LLMs (columns) and datasets (rows). Our work (vLiteRAG) achieves higher SLO attainment across all regimes compared to baselines, especially under high-load conditions and larger vector index.

approach, we also compare against HeteRAG [10] in section VIII-D, which also uses a skew-aware caching strategy.

VIII. Evaluations

A. Performance Model and Hit Rate Estimator

Figure 10 evaluates the accuracy of VectorLiteRAG's performance model. The right panel compares the predicted and actual minimum hit rates within each batch. The close alignment confirms that our Beta-distribution-based approximation reliably captures caching effectiveness.

As expected from order statistics, the minimum hit rate declines rapidly with increasing batch size, with the rate of decline flattening in the larger batch region.

The left panel compares the predicted latency of hybrid index search against the measured latency. While the predictions follow the same trend, there is a consistent offset between the two. This discrepancy primarily stems from the dispatcher's early query handling, which we discuss further in Section VIII-E. Despite this, the model serves as a reliable upper bound for search latency and is sufficiently accurate for guiding the partitioning algorithm.

B. SLO Attainment

Achieving service level objectives for TTFT across a wide range of input traffic is the primary goal of VectorLiteRAG. Figure 9 presents the SLO attainment curves across all nine combinations of vector databases and LLMs evaluated. In each subplot, the horizontal dashed line marks the 90th percentile latency target, while the vertical dashed line indicates the standalone LLM throughput. All experiments use an on-demand dynamic batching framework, where retrieval requests are served as soon as the previous search completes.

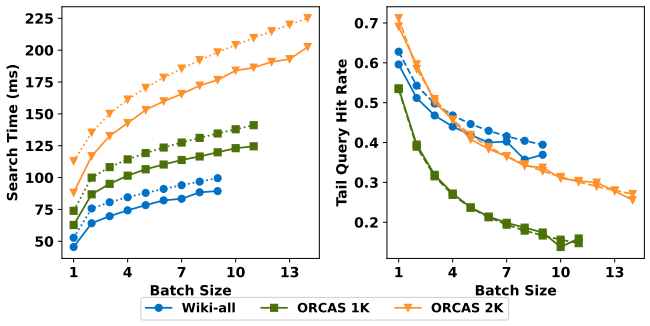

Fig. 10. Comparison of measured versus estimated values from VectorLiteRAG's performance model. **Left:** Predicted and actual search latency across batch sizes. **Right:** Estimated and measured minimum (tail) hit rates within a batch. The model accurately tracks trends and serves as a reliable upper bound for latency-aware partitioning.

This batching mechanism scales throughput with arrival rate by adapting batch sizes dynamically.

Across all configurations, VectorLiteRAG consistently sustains the extended SLO budget ($SLO_{\text{LLM}} + SLO_{\text{Search}}$, defined in Table I) over the widest input rate ranges among evaluated baselines. CPU-based fast scan can support relatively high request per second (RPS) rates, its limited per-request performance leads to consistent SLO violations even under light traffic. As arrival rate increases, batch sizes grow (up to 9–10 under >40 RPS), incurring high search latency and poor tail response.

Dedicated GPU retrieval performs poorly with large models due to rigid model parallelism constraints. For instance, Llama3-70B requires a tensor parallelism degree of 4 for efficient execution. While it fits within 2 H100 GPUs, the

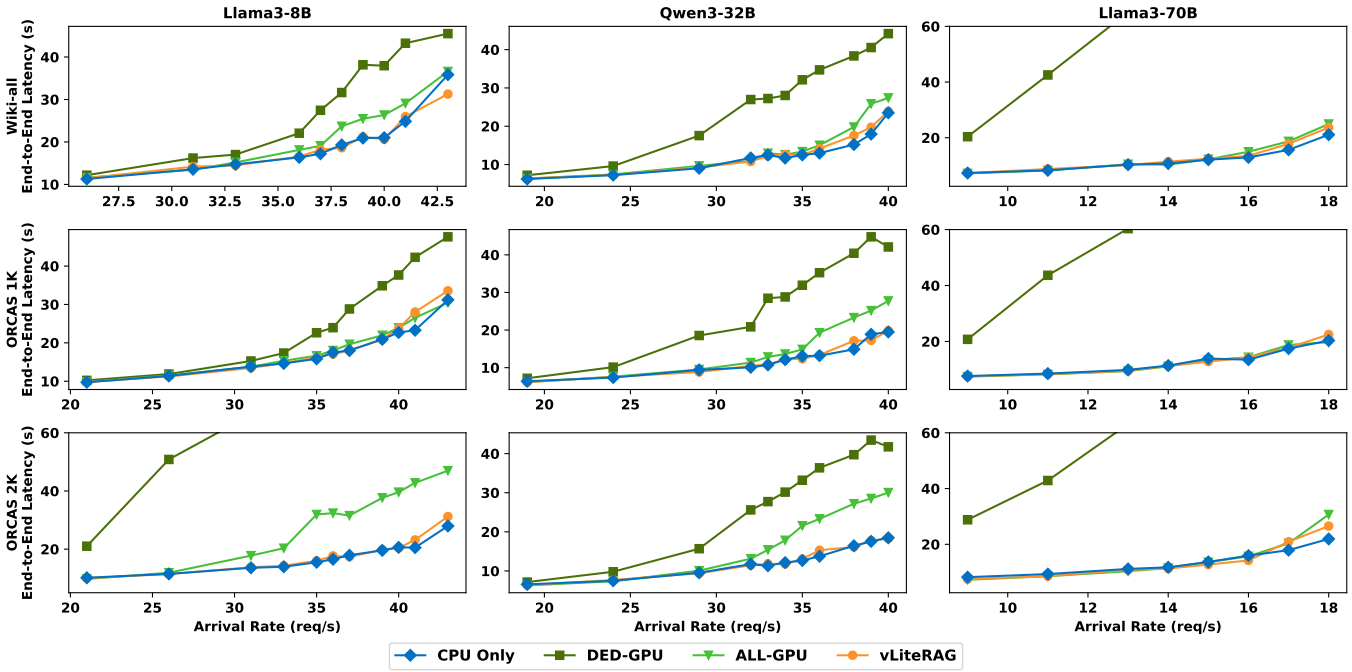

Fig. 11. End-to-end latency of the full RAG pipeline under varying arrival rates for different datasets. Compared systems include CPU-only retrieval (blue), dedicated GPU for retrieval (green triangle), all-GPU (green square), and vLiteRAG (orange) just as SLO attainment. vLiteRAG consistently maintains lower or comparable latency under high load conditions.

achievable LLM throughput drops from 8 RPS to less than 2 RPS. In such settings, dedicating GPU(s) to retrieval results in resource oversubscription, harming overall system throughput.

For small vector databases and under light loads, all-GPU shared configurations can satisfy SLOs over wide traffic ranges. However, as arrival rate approaches the reduced LLM throughput, due to index memory contention latency increases sharply. Although VECTORLITERAG is subject to this limitation as well, its optimized partitioning algorithm extends the SLO-attainable region nearly up to the standalone LLM throughput limit.

To better illustrate the dynamics of RAG systems, we present a detailed TTFT breakdown in Figure 12 for the Qwen3-32B model with Wiki-All and ORCAS 1K indices under varying input rates. As search latency increases, especially with CPU-based retrieval, queuing delays compound, further inflating TTFT. While both dedicated and all-GPU shared baselines perform well under low traffic, they exhibit latency spikes at higher rates due to resource contention. In contrast, VECTORLITERAG sustains stable latency by balancing throughput and latency, enabling finer control over resource allocation across the RAG stages.

C. End-to-End Latency

Since GPU resources are shared between retrieval and generation, interference with the decoding phase is inevitable. To assess the impact of such interference, we present the end-to-end latency results from the nine configurations discussed earlier, shown in Figure 11.

In the low-traffic regime, GPU resource contention is minimal, except in cases where dedicated GPUs are allocated solely

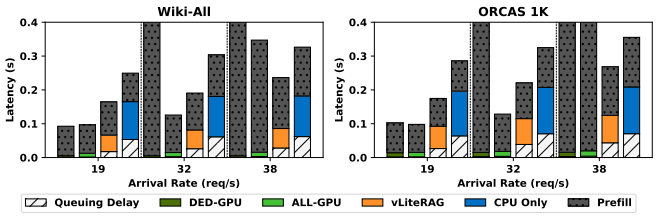

Fig. 12. TTFT latency breakdown for systems using the Wiki-All and ORCAS 1K indexes with Qwen3-32B. Each group shows results from four configurations: DED-GPU, All-GPU, VECTORLITERAG, and CPU-Only (from left to right). Bars are stacked to show the contribution of queuing delay, vector search latency (colored segments), and LLM prefill latency (grey)

for retrieval. However, under high traffic and with large vector databases, contention becomes significant. This is evident in the more than 2× increase in end-to-end latency observed in the all-GPU baselines for ORCAS 2K with Llama3-8B and Qwen3-32B. Although Llama3-70B involves more intensive computation, its low throughput ceiling causes TTFT to diverge before retrieval-induced interference becomes the dominant factor.

In contrast, VECTORLITERAG matches CPU-based retrieval in end-to-end latency. This demonstrates that its partitioning strategy and distributed pipeline effectively minimizes interference by carefully limiting GPU memory and compute usage for retrieval, thereby preserving LLM generation performance.

D. Comparison with HeterRAG

In this section, we compare VECTORLITERAGwith HeterRAG [10], that also exploits skewed cluster access patterns in RAG pipelines. While both systems adopt tiered caching

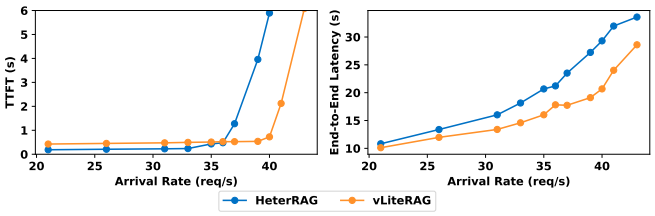

Fig. 13. Comparison with HeterRAG. While HeterRAG achieves lower TTFT initially, its latency increases beyond the throughput-bound caching limit. VECTORLITERAG is configured with $SLO_{search} = 400$ms.

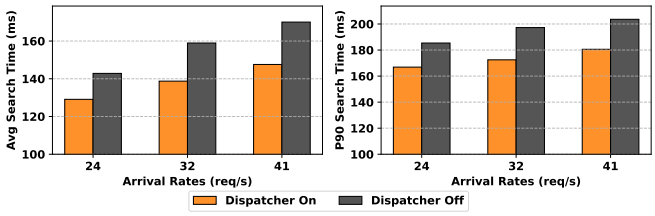

Fig. 14. **Left:** Vector search average and **Right:** P90 tail latency on ORCAS 2K index with dispatcher enabled and disabled.

strategies for vector index, their partitioning principles and system targets differ fundamentally.

HeterRAG selects GPU-resident clusters by identifying the maximum KV cache size that can sustain the throughput of the slower stage, either the LLM or the retriever. While this approach is simple and throughput-aware, it is inflexible to latency constraints that are critical for real-time serving. In configurations where the LLM stage exhibits lower peak throughput than retrieval, as in our main evaluations, HeterRAG allocates the entire GPU memory to LLMs, leaving vector search to be performed on the CPU. As stated in their paper, the benefit of HeterRAG's scheme primarily applies to scenarios where retrieval becomes extremely heavy.

To provide a fair comparison, we replicated the HeterRAG setting by building an IVF index with the number of clusters set to $\sqrt{N_{\text{vector}}}$ and measured retrieval throughput using batch sizes below 64. At `nprobe` $= 256$, CPU-only retrieval achieves 35 RPS at 0.94 NDCG@50. `nprobe` in our system is increased accrodingly to 6144 to match this accuracy level. We implemented both systems using their respective partitioning policies. Since HeterRAG does not support distributed retrieval, we applied their GPU caching scheme using `IndexIVFShard` without our optimized pipeline.

Figure 13 summarizes the results. HeterRAG places 73% of the index clusters in GPU memory, whereas VECTORLITERAG identifies a partitioning point at 31.5% of clusters under a 400ms SLO constraint. HeterRAG achieves lower retrieval latency under low traffic, but its operable region is limited as input rates increase. VECTORLITERAG maintains latency around the specified constraint across a wider range of traffic levels. In addition, thanks to efficient resource usage in our distributed pipeline it also achieves lower end-to-end latency overall through its optimized, distributed retrieval pipeline.

The key difference lies in how partitioning decisions are made. VECTORLITERAG enables the system operator to specify a target SLO and computes the largest feasible GPU-resident index region that meets this constraint. In contrast, HeterRAG determines partitioning solely based on balancing throughput between stages, without considering latency objectives. As a result, it lacks fine-grained latency control and may misallocate GPU resources.

E. Dynamic Dispatcher

Figure 14 illustrates the effectiveness of the dynamic dispatcher in the VECTORLITERAG pipeline. By polling the scanning loop and dispatching queries as soon as they complete, the dispatcher reduces search latency by up to 16%. This optimization benefits not only the average latency, but also the tail latency, as shown in the right pane of the figure. The improvement comes from overlapping the merging and re-ranking of early-completed queries with the ongoing scanning of slower queries, thereby alleviating the overhead of merging all results in bulk at the end.

IX. RELATED WORKS

RAG applications with iterative retrieval or multi-stage generation often exhibit semantic similarity across successive queries. Motivated by this observation, several optimization techniques have been proposed, including prefetching [22], speculative retrieval [41], and pipelined execution [14]. In contrast, our work builds upon application-agnostic, generic retrieval–generation pipelines without relying on semantic priors or intermediate signals.

RagCache [15] improves the generation throughput by managing the reuse of KV cache between tenants, focusing on scheduling on the LLM side. Hermes [33] achieves datacenter-scale throughput by offloading vector search to additional CPU nodes, at the cost of requiring disaggregated infrastructure.

Efforts like [11], [13], [20], [24], [30] propose specialized hardware or memory centric architectures to accelerate RAG pipelines. While these approaches offer significant performance gains, they often rely on custom infrastructure, which may limit deployability in general-purpose environments.

Among prior works, HeterRAG [10] also co-locates retrieval and generation on GPU. Our work builds on this direction with an analytical model for latency and hitrate, enabling principled GPU memory partitioning under explicit SLOs. To our knowledge, VECTORLITERAG is the first solution offering fine-grained resource control for co-located RAG pipelines.

X. CONCLUSION

This paper presents VECTORLITERAG, a latency-aware resource sharing framework for RAG systems, along with an optimized and distributed execution pipeline. VECTORLITERAG achieves SLO compliance over a wider range of input traffic, handling up to 1.5× higher input traffic while meeting the target latency. As a deployable system, it offers RAG service providers fine-grained control over GPU resource

allocation, enabling them to balance throughput and latency under constrained GPU memory budgets.

REFERENCES

[1] M. Adnan, Y. E. Maboud, D. Mahajan, and P. J. Nair, "Accelerating recommendation system training by leveraging popular choices," *Proc. VLDB Endow.*, vol. 15, no. 1, p. 127–140, sep 2021.

[2] M. Adnan, Y. E. Maboud, D. Mahajan, and P. J. Nair, "Heterogeneous acceleration pipeline for recommendation system training," in *2024 ACM/IEEE 51st Annual International Symposium on Computer Architecture (ISCA)*. IEEE, 2024, pp. 1063–1079.

[3] F. André, A.-M. Kermarrec, and N. Le Scouarnec, "Cache locality is not enough: High-performance nearest neighbor search with product quantization fast scan," in *42nd International Conference on Very Large Data Bases*, vol. 9, no. 4, 2016, p. 12.

[4] N. Craswell, D. Campos, B. Mitra, E. Yilmaz, and B. Billerbeck, "Orcas: 18 million clicked query-document pairs for analyzing search," *arXiv preprint arXiv:2006.05324*, 2020.

[5] M. Douze, A. Guzhva, C. Deng, J. Johnson, G. Szilvasy, P.-E. Mazaré, M. Lomeli, L. Hosseini, and H. Jégou, "The faiss library," *arXiv preprint arXiv:2401.08281*, 2024.

[6] A. Dubey, A. Jauhri, A. Pandey, A. Kadian, A. Al-Dahle, A. Letman, A. Mathur, A. Schelten, A. Yang, A. Fan *et al.*, "The llama 3 herd of models," *arXiv e-prints*, pp. arXiv–2407, 2024.

[7] W. Fan, Y. Ding, L. Ning, S. Wang, H. Li, D. Yin, T.-S. Chua, and Q. Li, "A survey on rag meeting llms: Towards retrieval-augmented large language models," in *Proceedings of the 30th ACM SIGKDD Conference on Knowledge Discovery and Data Mining*, 2024, pp. 6491–6501.

[8] Y. Gao, Y. Xiong, X. Gao, K. Jia, J. Pan, Y. Bi, Y. Dai, J. Sun, and H. Wang, "Retrieval-augmented generation for large language models: A survey," *arXiv preprint arXiv:2312.10997*, 2023.

[9] K. Guu, K. Lee, Z. Tung, P. Pasupat, and M. Chang, "Retrieval augmented language model pre-training," in *International conference on machine learning*. PMLR, 2020, pp. 3929–3938.

[10] Z. Hu, V. Murthy, Z. Pan, W. Li, X. Fang, Y. Ding, and Y. Wang, "Hedrarag: Coordinating llm generation and database retrieval in heterogeneous rag serving," *arXiv preprint arXiv:2507.09138*, 2025.

[11] J. Jang, H. Choi, H. Bae, S. Lee, M. Kwon, and M. Jung, "Cxl-anns:software-hardware collaborative memory disaggregation and computation for billion-scale approximate nearest neighbor search," in *2023 USENIX Annual Technical Conference (USENIX ATC 23)*, 2023, pp. 585–600.

[12] H. Jegou, M. Douze, and C. Schmid, "Product quantization for nearest neighbor search," *IEEE transactions on pattern analysis and machine intelligence*, vol. 33, no. 1, pp. 117–128, 2010.

[13] W. Jiang, M. Zeller, R. Waleffe, T. Hoefler, and G. Alonso, "Chameleon: a heterogeneous and disaggregated accelerator system for retrieval-augmented language models," *arXiv preprint arXiv:2310.09949*, 2023.

[14] W. Jiang, S. Zhang, B. Han, J. Wang, B. Wang, and T. Kraska, "Piperag: Fast retrieval-augmented generation via algorithm-system co-design," *arXiv preprint arXiv:2403.05676*, 2024.

[15] C. Jin, Z. Zhang, X. Jiang, F. Liu, X. Liu, X. Liu, and X. Jin, "Ragcache: Efficient knowledge caching for retrieval-augmented generation," *arXiv preprint arXiv:2404.12457*, 2024.

[16] J. Johnson, M. Douze, and H. Jégou, "Billion-scale similarity search with GPUs," *IEEE Transactions on Big Data*, vol. 7, no. 3, pp. 535–547, 2019.

[17] W. Kwon, Z. Li, S. Zhuang, Y. Sheng, L. Zheng, C. H. Yu, J. Gonzalez, H. Zhang, and I. Stoica, "Efficient memory management for large language model serving with pagedattention," in *Proceedings of the 29th Symposium on Operating Systems Principles*, 2023, pp. 611–626.

[18] Y. Kwon and M. Rhu, "Training personalized recommendation systems from (gpu) scratch: Look forward not backwards," in *Proceedings of the 49th Annual International Symposium on Computer Architecture*, 2022, pp. 860–873.

[19] LangChain-Team, "Langchain: Context-aware reasoning framework," https://github.com/langchain-ai/langchain, 2025, accessed: 2025-07-24.

[20] Y. Lee, H. Choi, S. Min, H. Lee, S. Beak, D. Jeong, J. W. Lee, and T. J. Ham, "Anna: Specialized architecture for approximate nearest neighbor search," in *2022 IEEE International Symposium on High-Performance Computer Architecture (HPCA)*. IEEE, 2022, pp. 169–183.

[21] P. Lewis, E. Perez, A. Piktus, F. Petroni, V. Karpukhin, N. Goyal, H. Küttler, M. Lewis, W.-t. Yih, T. Rocktäschel *et al.*, "Retrieval-augmented generation for knowledge-intensive nlp tasks," *Advances in neural information processing systems*, vol. 33, pp. 9459–9474, 2020.

[22] C.-Y. Lin, K. Kamahori, Y. Liu, X. Shi, M. Kashyap, Y. Gu, R. Shao, Z. Ye, K. Zhu, S. Wang *et al.*, "Telerag: Efficient retrieval-augmented generation inference with lookahead retrieval," *arXiv preprint arXiv:2502.20969*, 2025.

[23] J. Liu, "Llamaindex," https://github.com/jerryjliu/llama_index, Nov. 2022, released on November 1, 2022. [Online]. Available: https://github.com/jerryjliu/llama_index

[24] R. Mahapatra, H. Santhanam, C. Priebe, H. Xu, and H. Esmaeilzadeh, "In-storage acceleration of retrieval augmented generation as a service," in *Proceedings of the 52nd Annual International Symposium on Computer Architecture*, 2025, pp. 450–466.

[25] Y. A. Malkov and D. A. Yashunin, "Efficient and robust approximate nearest neighbor search using hierarchical navigable small world graphs," *IEEE transactions on pattern analysis and machine intelligence*, vol. 42, no. 4, pp. 824–836, 2018.

[26] S. Merity, C. Xiong, and R. Socher, "Pointer sentinel mixture models," *arXiv preprint arXiv:1609.07843*, 2016.

[27] D. Mudigere, Y. Hao, J. Huang, Z. Jia, A. Tulloch, S. Sridharan, X. Liu, M. Ozdal, J. Nie, J. Park *et al.*, "Software-hardware co-design for fast and scalable training of deep learning recommendation models," in *Proceedings of the 49th Annual International Symposium on Computer Architecture*, 2022, pp. 993–1011.

[28] A. Neelakantan, T. Xu, R. Puri, A. Radford, J. M. Han, J. Tworek, Q. Yuan, N. Tezak, J. W. Kim, C. Hallacy *et al.*, "Text and code embeddings by contrastive pre-training," *arXiv preprint arXiv:2201.10005*, 2022.

[29] P. Patel, E. Choukse, C. Zhang, A. Shah, Í. Goiri, S. Maleki, and R. Bianchini, "Splitwise: Efficient generative llm inference using phase splitting," in *2024 ACM/IEEE 51st Annual International Symposium on Computer Architecture (ISCA)*. IEEE, 2024, pp. 118–132.

[30] D. Quinn, M. Nouri, N. Patel, J. Salihu, A. Salemi, S. Lee, H. Zamani, and M. Alian, "Accelerating retrieval-augmented generation," in *Proceedings of the 30th ACM International Conference on Architectural Support for Programming Languages and Operating Systems, Volume 1*, 2025, pp. 15–32.

[31] O. Ram, Y. Levine, I. Dalmedigos, D. Muhlgay, A. Shashua, K. Leyton-Brown, and Y. Shoham, "In-context retrieval-augmented language models," *Transactions of the Association for Computational Linguistics*, vol. 11, pp. 1316–1331, 2023.

[32] N. Reimers, "Sentence-bert: Sentence embeddings using siamese bert-networks," *arXiv preprint arXiv:1908.10084*, 2019.

[33] M. Shen, M. Umar, K. Maeng, G. E. Suh, and U. Gupta, "Hermes: Algorithm-system co-design for efficient retrieval-augmented generation at-scale," in *Proceedings of the 52nd Annual International Symposium on Computer Architecture*, 2025, pp. 958–973.

[34] K. Song, X. Tan, T. Qin, J. Lu, and T.-Y. Liu, "Mpnet: Masked and permuted pre-training for language understanding," *Advances in neural information processing systems*, vol. 33, pp. 16 857–16 867, 2020.

[35] R. A. Team, "Wiki-all dataset," https://docs.rapids.ai/api/cuvs/stable/cuvs_bench/wiki_all_dataset/, 2024, accessed: 2025-07-31.

[36] J. Wang, X. Yi, R. Guo, H. Jin, P. Xu, S. Li, X. Wang, X. Guo, C. Li, X. Xu *et al.*, "Milvus: A purpose-built vector data management system," in *Proceedings of the 2021 International Conference on Management of Data*, 2021, pp. 2614–2627.

[37] Y. Wang, L. Wang, Y. Li, D. He, and T.-Y. Liu, "A theoretical analysis of ndcg type ranking measures," in *Conference on learning theory*. PMLR, 2013, pp. 25–54.

[38] A. Yang, A. Li, B. Yang, B. Zhang, B. Hui, B. Zheng, B. Yu, C. Gao, C. Huang, C. Lv *et al.*, "Qwen3 technical report," *arXiv preprint arXiv:2505.09388*, 2025.

[39] D. Zhang, J. Li, Z. Zeng, and F. Wang, "Jasper and stella: distillation of sota embedding models," *arXiv preprint arXiv:2412.19048*, 2024.

[40] J. Zhang, Q. Liu, D. Lian, Z. Liu, L. Wu, and E. Chen, "Anisotropic additive quantization for fast inner product search," in *Proceedings of the AAAI conference on Artificial Intelligence*, vol. 36, no. 4, 2022, pp. 4354–4362.

[41] Z. Zhang, A. Zhu, L. Yang, Y. Xu, L. Li, P. M. Phothilimthana, and Z. Jia, "Accelerating retrieval-augmented language model serving with speculation," *arXiv preprint arXiv:2401.14021*, 2024.

[42] Y. Zhong, S. Liu, J. Chen, J. Hu, Y. Zhu, X. Liu, X. Jin, and H. Zhang, "Distserve: Disaggregating prefill and decoding for goodput-optimized large language model serving," in *18th USENIX Symposium on Operating Systems Design and Implementation (OSDI 24)*, 2024, pp. 193–210.

[43] J. Zobel and A. Moffat, "Inverted files for text search engines," *ACM computing surveys (CSUR)*, vol. 38, no. 2, pp. 6–es, 2006.